This paper is available on line at http://www.mcponline.org

Platelet Proteome Analysis Reveals Integrin-dependent Aggregation Defects in Patients with Myelodysplastic Syndromes*[S]

Julia Fröbel‡§¶, Ron-Patrick Cadeddu§, Sonja Hartwig¶, Ingmar Bruns§, Christian M. Wilk§, Andrea Kündgen§, Johannes C. Fischer‖, Thomas Schroeder§, Ulrich G. Steidl, Ulrich Germing§, Stefan Lehr¶, Rainer Haas§, and Akos Czibere§**

Bleeding complications are a significant clinical problem in patients with myelodysplastic syndromes even at sufficient platelet counts (>50,000/μl). However, the underlying pathology of this hemorrhagic diathesis is still unknown. Here, we analyzed the platelet proteome of patients with myelodysplastic syndromes by quantitative two-dimensional difference gel electrophoresis followed by mass spectrometric protein identification. Proteins identified with lower concentrations, such as Talin-1, Vinculin, Myosin-9, Filmain-A, and Actin play critical roles in integrin $\alpha_{IIb}\beta_3$ signaling and thus platelet aggregation. Despite normal agonist receptor expression, calcium flux, and granule release upon activation, the activation capacity of integrin $\alpha_{IIb}\beta_3$ was diminished in myelodysplastic syndrome platelets. Förster resonance energy transfer analysis showed a reduced co-localization of Talin-1 to the integrin's β_3-subunit, which is required for receptor activation and fibrinogen binding. In addition, platelet spreading on immobilized fibrinogen was incomplete, and platelet aggregation assays confirmed a general defect in integrin-dependent platelet aggregation in patients with myelodysplastic syndromes. Our data provide novel aspects on the molecular pathology of impaired platelet function in myelodysplastic syndromes and suggest a mechanism of defective integrin $\alpha_{IIb}\beta_3$ signaling that may contribute to the hemorrhagic diathesis observed in these patients. ***Molecular & Cellular Proteomics 12: 10.1074/mcp.M112.023168, 1272–1280, 2013.***

Myelodysplastic syndromes (MDS)[1] are among the most frequent hematological malignancies (1). Each of the hematopoietic lineages may be affected by dysplasia and/or cytopenia, and patients suffering from this clonal bone marrow disease are affected by anemia and infectious as well as hemorrhagic complications (1, 2). Thrombocytopenia itself is prevalent in up to 65% of patients with MDS at the time of diagnosis (3). Recently, a detailed study of the clinical features of 2900 patients with MDS reported that even among patients with platelet counts of >50,000/μl, 19% had signs of bleeding at the time of diagnosis (4). Taken together, these data suggest a platelet count-independent functional platelet defect in MDS, which is supported by sporadic reports indicating insufficient platelet aggregation (3, 5–8). The existence of such a functional platelet defect may very well contribute to the high rate of hemorrhagic complications observed in patients with MDS.

Platelet aggregation following a vascular injury or other stimuli is a highly organized process to ensure optimal efficacy. Exposure to collagen, von Willebrand factor, or soluble platelet agonists such as ADP, thrombin, or thromboxane A_2 at the site of injury attracts platelets and initiates platelet adhesion. This activates and recruits additional platelets from the blood to finally cover the injury (9, 10). The fibrinogen receptor (integrin $\alpha_{IIb}\beta_3$) plays an essential role in this process (10–13). On resting platelets, integrin $\alpha_{IIb}\beta_3$ resides in a low affinity state and depends on intrinsic signals for activation and function (14). The final step in this activation process is the co-localization of Talin-1 from the cytoplasm to the β-subunit of the integrin (12, 13, 15, 16). Once activated, $\alpha_{IIb}\beta_3$ is linked to the actin cytoskeleton by several linker proteins, which is required for platelet aggregation and spreading (12, 17, 18). Hence, a series of key proteins like Talin-1, Kindlin-3, Vinculin, Actin, and Myosin-9 need to be expressed in platelets for sufficient integrin $\alpha_{IIb}\beta_3$ function and hemostasis. Despite some evidence that a functional platelet defect may exist in MDS, no data are yet available to explain the hemorrhagic diathesis in those patients who present with sufficient platelet counts. In this study, we performed a comprehensive analysis

From the Departments of §Hematology, Oncology, and Clinical Immunology and ¶Clinical Biochemistry and Pathobiochemistry, Leibniz Center for Diabetes Research, and ‖Institute for Transplantation Diagnostics and Cell Therapeutics, Heinrich-Heine-University, 40225 Düsseldorf, Germany and the **Department of Cell Biology and Albert Einstein Cancer Center, Albert Einstein College of Medicine, Bronx, New York 10461

Received August 21, 2012, and in revised form, January 28, 2013
Published, MCP Papers in Press, February 4, 2013, DOI 10.1074/mcp.M112.023168

[1] The abbreviations used are: MDS, myelodysplastic syndrome; PE, phycoerythrin; APC, allophycocyanin; TRAP, thrombin receptor activating peptide, CD, cluster of differentiation; MFI, mean fluorescence intensity.

of the platelet proteome of MDS patients and MDS platelet aggregation. We show that the critical integrin $\alpha_{IIb}\beta_3$ is functionally impaired and that a series of proteins essential for its proper function have a reduced expression in MDS.

EXPERIMENTAL PROCEDURES

Patient Characteristics—The 66 MDS patients included into this study had a median age of 66 years and a median platelet count of 100,000/μl and did not receive platelet transfusion or any medication possibly interfering with platelet function. Please note that not all patient samples were used in each experiment, and for detailed patient characteristics and application to the single experiments, see supplemental Table S1. Informed consent was obtained according to a protocol approved by the ethics committee of the Heinrich-Heine-University, Düsseldorf, Germany.

Platelet Preparation—Platelets were prepared according to a standard operating procedure of the Heinrich-Heine-University Clinic. Citrate-anticoagulated peripheral blood was centrifuged for 30 min at 150 $\times$ *g* to obtain platelet-rich plasma. Platelets were isolated from platelet-rich plasma by a 10-min centrifugation at 300 $\times$ *g*, washed, and stored in modified Tyrode's/Hepes buffer (12). The purity of the samples for residual leukocytes and erythrocytes was checked by flow cytometry.

Two-dimensional Difference Gel Electrophoresis—Platelets of seven MDS patients and seven normal donors were lysed (7 M urea, 2 M thiourea, 25 mM Tris, 4% CHAPS, protease, and phosphatase inhibitors), sonicated, and centrifuged (60 min, 35,000 $\times$ *g*, 4 °C). The protein concentration of the supernatants was determined by protein assay according to the manufacturer's instructions (Bio-Rad). Fluorescence labeling of the single lysates with cyanine dyes was done as recommended by the manufacturer (GE Healthcare). To eliminate dye-specific differences, 1 aliquot of each sample was labeled with Cy3 and one with Cy5 (dye-swap). An internal standard for all 14 two-dimensional gels consisting of equal protein amounts of all 14 samples was labeled with Cy2. Three samples (each 50 μg of protein of the internal standard labeled with Cy2, one MDS patient labeled with Cy3, and one healthy donor labeled with Cy5 or vice versa) were combined per gel and applied to Immobiline™ DryStrips (GE Healthcare) by cup loading. Isoelectric focusing was performed on a MultiPhor II (GE Healthcare) as described previously (19). The strips were then loaded onto linear 12.5% polyacrylamide gels, and second dimension separation was performed using a Laemmli buffer system on an EttanDalt 12 system (GE Healthcare) as described previously (19).

Gel Imaging and Analysis—Gels were scanned using a Typhoon 9400 (GE Healthcare), and protein spot abundances and statistics were determined by Proteomweaver 4.0 (Bio-Rad). Gel images were grouped for comparison. Images of the 14 internal standard gels were combined in group 1, and group 2 contained the 14 images of all normal donor samples. Each of the seven patients comprised an individual group containing the two dye-swap gel images. All gel images were matched automatically and normalized using the internal standard (labeled in Cy2). Significantly changed protein spots were determined by the following three-step procedure: 1) the spot was matched across at least 10 of 14 gels; 2) its standardized average spot volume ratio exceeded 1.5 in at least five of the seven patients compared with the normal donor group, and 3) this change in spot volume was statistically significant ($p < 0.05$).

Protein Identification and Pathway Analysis—Protein spots of interest were excised from the gels using a Gelpix spot picker (Genetix). Gel pieces were washed and proteins trypsin-digested, and the resulting peptides were eluted as depicted before (19) and applied to a MALDI Prespotted AnchorChip target (Bruker Daltonics). Samples were analyzed in an Ultraflex-Tof/Tof mass spectrometer, and acquired mass spectra were annotated using Compass 1.3 software (both from Bruker Daltonics). All spectra were re-calibrated internally using the mass-list generated by Bruker Daltonics (based on 400 identified spectra to assign laboratory-specific peaks that should be excluded, see supplemental Data S1). Protein identification was performed using Biotools 3.2 (Bruker Daltonics) by searching SwissProt (SwissProt_57.12.fasta, 513877 sequences) and NCBInr (NCBInr_20090324.fasta, 8097822 sequences) databases with Mascot 2.2.04 (Matrix Science) using the following search parameters: enzyme "trypsin," species "human," fixed modifications "carbamidomethyl," optional modifications "methionine oxidation," missed cleavages "1," and mass tolerance "50 ppm." Calculated pI and molecular mass data were obtained by Mascot. For peptides matching different isoforms or multiple members of a protein family, we used the following reporting criteria. The experimental pI and molecular mass taken from the two-dimensional gels were compared with the theoretical data of the different isoforms/protein members. If no conflicts in molecular mass or pI were found, the isoform/protein member with the highest mascot score was reported. Proteins were considered as identified with a Mascot score of >56 ($p < 0.05$) on at least two physically different gels. Pathway and signaling network analysis was performed by Ingenuity Pathway Analysis tools (Ingenuity Systems).

Western Blot Analysis—The pooled platelet lysates of the seven MDS patients and seven normal donors were separated by SDS-PAGE, blotted onto a PVDF membrane, and incubated with appropriate antibodies followed by nitro blue tetrazolium/5-bromo-4-chloro-3-indolyl phosphate (Roche Applied Science) development. Antibodies used were mouse anti-human-talin-1 (LSBio; 1:2500), rabbit anti-human-MYH9 (Sigma-Aldrich; 1:500), mouse anti-human-vinculin, and mouse anti-human-filamin-A (both Abcam; 1:2500). Secondary antibodies were AP-conjugated donkey anti-mouse and donkey anti-rabbit (both Abcam; 1:2500). Rabbit anti-human-β-tubulin (Abcam; 1:2500) was used as loading control. Bands were quantified by pixel intensity using ImageJ software (rsbweb.nih.gov).

Förster Resonance Energy Transfer (FRET)—Washed platelets from five MDS patients and normal donors were incubated with 1 unit/ml thrombin and simultaneously stained for 20 min at RT in the dark with anti-CD41 (Acris Antibodies) and anti-talin-1 (LSBio) conjugated to phycoerythrin (PE) and allophycocyanin (APC) using Lynx Rapid Conjugation kits (AbD Serotec). FRET was measured using a Cytomics FC500 flow cytometer (Beckman Coulter) equipped with 488- and 635-nm lasers. If the APC-labeled talin-1 probe was in close physical proximity (<10 nm) to the 488-nm excited PE-labeled integrin, it absorbed the energy emitted at 575 nm and emitted light at 675 nm without the use of the 635-nm laser. The increase in the MFI at 675 nm was recorded to quantify co-localization of talin-1 and the integrin. All samples were checked for sufficient staining prior to FRET analysis.

Whole Blood Flow Cytometry—Within 30 min after blood sampling, 10 μl of citrate-anticoagulated whole blood from 11 MDS patients and normal donors was diluted in PBS, incubated with agonists, simultaneously stained with antibodies for 20 min at RT in the dark, and subsequently analyzed using a FACSCalibur (BD Biosciences). Agonists used were 5×10^{-6} M thrombin receptor-activating peptide (TRAP), 10^{-5} M phorbol 12-myristate 13-acetate, and 10^{-3} M $MnCl_2$. Antibodies used were anti-CD41-FITC (clone P2, Acris Antibodies), goat anti-human GPVI (Santa Cruz Biotechnology), rabbit anti-human $P2Y_1$ and $P2Y_{12}$ (Alomone Labs), and PAC-1-FITC, CD42b-PE, CD49b-PE, CD61-PE, CD62P-APC, and isotype controls (all from BD Biosciences). Unconjugated antibodies were stained with AF488-conjugated goat anti-rabbit or rabbit anti-goat secondary antibodies (Invitrogen). Cytosolic free calcium concentration ($[Ca^{2+}]_i$) of the platelets of 10 MDS patients and normal donors was measured upon

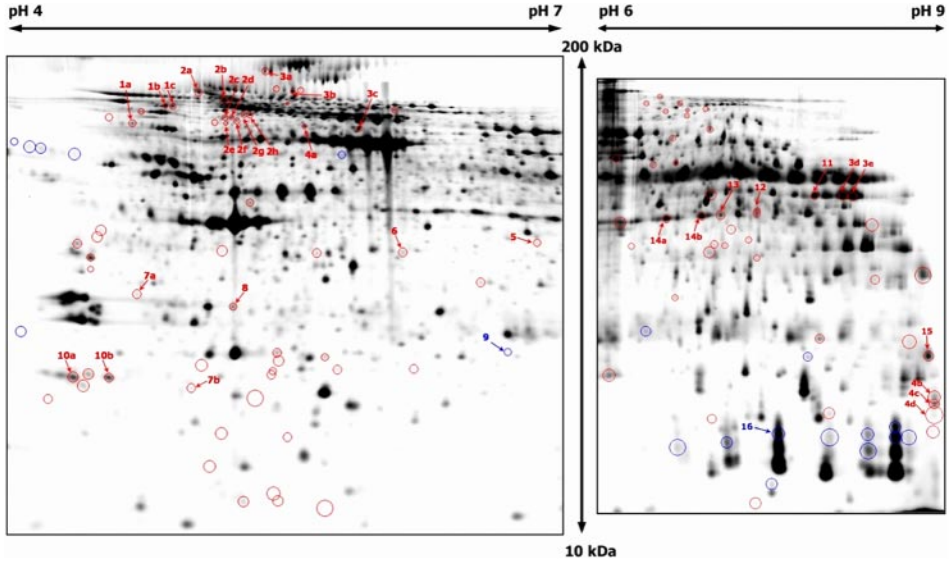

FIG. 1. **Differential proteome analysis of normal donor and MDS platelets.** Representative two-dimensional gel image of platelet lysates (pH ranges 4–7 and 6–9) showing the 120 protein spots with different concentrations between the seven MDS patients and seven normal donors analyzed. *Red circles* represent the 101 spots with lower levels in MDS platelets, and *blue circles* represent the 19 spots with higher levels in MDS platelets. The serial numbers are identical to the numbers given in Table I, showing the position of each of the identified proteins. *Letters* following numbers are used to distinguish between different spots representing the same protein.

activation with 50 mM ADP or 1 unit/ml thrombin using whole blood diluted 1:10 in calcium-free PBS and incubated with 10 μM Fluo-4AM (Invitrogen) for 20 min at 37°C in the dark.

Aggregometry—Aggregometry of 58 MDS patients and 10 normal donors was performed according to a standard operation procedure at the Department of Clinical Chemistry and Laboratory Diagnostics, Heinrich-Heine-University Clinic. Within 2 h after blood collection, platelet-rich plasma was isolated and stimulated with 20 μM ADP, 0.5 mg/ml arachidonic acid, 10 μg/ml collagen, or 1.5 mg/ml ristocetin. Light transmission was recorded on a platelet aggregation profiler PAP8 (möLab) over 20 min.

Platelet Spreading Experiments—Glass-bottom dishes (MatTek) were coated with 1 mg/ml human fibrinogen and blocked with 1% BSA in PBS. BSA-coated dishes were used as controls. Washed platelets of four MDS patients and normal donors were seeded at a concentration of $0.5 \times 10^6/\mu$l, activated with 1 unit/ml thrombin, and analyzed by differential interference contrast microscopy over 30 min.

Statistical Analysis—Frequency tables (*z*-test) and mean comparison (*t* test) were used for statistical examination. P values are given in the text and stars are used throughout the figures to indicate the level of significance (*$p<0.05$, **$p<0.01$, ***$p<0.001$). No corrections for multiple hypothesis testing were performed to allow for maximum detection of potentially differentially expressed proteins. Established methods for correction lowered the number of false-positive discoveries at the expense of increasing false-negative discoveries. χ^2 automatic interaction detection was used for modeling the dependence of the aggregation defect on multiple clinical parameters (all SPSS 19, IBM).

RESULTS

Platelet Proteome Analysis Reveals Low Levels of Proteins Critical for Integrin Receptor Signaling and Platelet Function—To gain insights into the molecular pathology of platelet dysfunctions in MDS, we conducted a comprehensive analysis of the entire MDS platelet proteome. We performed two-dimensional difference gel electrophoresis for a quantitative comparison of platelet lysates obtained from seven MDS patients and seven normal donors. We detected a total number of 1649 protein spots of which 120 spots (7%) significantly differed between MDS and normal donor platelets regarding their concentration (Fig. 1). Among the differentially expressed protein spots, 101 spots (84%) had a lower expression in MDS platelets. We identified 35 of the differentially expressed protein spots (29%) representing 16 distinct proteins (Table I). Whereas nine protein species were identified from one spot each, seven protein species could be identified from more than one spot indicating different post-translational modification statuses of these proteins. The fold changes of these proteins discovered in more than one spot had similar values in the same direction. Ten of the 16 proteins (Talin-1, Kindlin-3, Vinculin, Filamin-A, Actin, Myosin-9, Myosin regulatory light chain 2 [MRLC2], Integrin-linked protein kinase [ILK], Cysteine and glycine-rich protein 1 [CSRP1], and Pleckstrin), all with lower levels in MDS, are involved in integrin $\alpha_{IIb}\beta_3$ signaling and function (see supplemental Data S1 for mass spectra and peptide coverage). The decreased expression of Talin-1, Myosin-9, Filamin-A, and Vinculin was also confirmed by Western blot showing a 23% decrease of Talin-1 amount in MDS platelets compared with healthy donor platelets as well as 42% of Vinculin, 17% of Filamin-A, and 63% of Myosin-9, respectively, although β-tubulin levels were not altered (Fig. 2). Subsequent ingenuity network and pathway analysis of the 16 identified proteins with altered expression in MDS revealed integrin signaling and cytoskeletal reorganization, both critical for platelet function, to be the most affected pathways (Fig. 3, *A* and *B*).

TABLE I
Identified proteins with differential expression in MDS

No.	Accession no.	Title of protein	Spot intensity healthy	Spot intensity MDS	FC	*p* value
1a	FLNA_HUMAN	Filamin-A	0.1254	0.0515	−2.43	0.000009
1b	FLNA_HUMAN	Filamin-A	0.2053	0.1004	−2.04	0.006578
1c	FLNA_HUMAN	Filamin-A	0.1310	0.0599	−2.19	0.003582
2a	MYH9_HUMAN	Myosin-9	0.0675	0.0257	−2.63	0.020416
2b	MYH9_HUMAN	Myosin-9	0.6042	0.3622	−1.67	0.004491
2c	MYH9_HUMAN	Myosin-9	0.5107	0.2604	−1.96	0.019720
2d	MYH9_HUMAN	Myosin-9	0.1421	0.0598	−2.38	0.013282
2e	MYH9_HUMAN	Myosin-9	0.1304	0.0572	−2.28	0.020173
2f	MYH9_HUMAN	Myosin-9	0.1026	0.0548	−1.87	0.025893
2g	MYH9_HUMAN	Myosin-9	0.1688	0.0805	−2.10	0.011641
2h	MYH9_HUMAN	Myosin-9	0.2767	0.1297	−2.13	0.003862
3a	TLN1_HUMAN	Talin-1	0.3525	0.1741	−2.02	0.013270
3b	TLN1_HUMAN	Talin-1	0.3283	0.1223	−2.69	0.019528
3c	TLN1_HUMAN	Talin-1	0.4103	0.2079	−1.97	0.000318
3d	TLN1_HUMAN	Talin-1	2.7395	1.3022	−2.10	0.000014
3e	TLN1_HUMAN	Talin-1	3.0228	1.4448	−2.09	0.000095
4a	VINC_HUMAN	Vinculin	0.1102	0.0364	−3.03	0.000000
4b	VINC_HUMAN	Vinculin	0.4126	0.1434	−2.88	0.000427
4c	VINC_HUMAN	Vinculin	0.4146	0.1396	−2.97	0.000285
4d	VINC_HUMAN	Vinculin	0.2606	0.0987	−2.64	0.001262
5	FIBP_HUMAN	Fibroblast growth factor-binding protein	0.0684	0.0272	−2.51	0.039802
6	URP2_HUMAN	Kindlin-3	0.0664	0.0321	−2.07	0.002287
7a	ACTG_HUMAN	Actin, cytoplasmic 2	0.0874	0.0403	−2.17	0.003818
7b	ACTB_HUMAN	Actin, cytoplasmic 1	0.1352	0.0473	−2.86	0.044098
8	CLIC1_HUMAN	Chloride intracellular channel protein 1	0.4149	0.0681	−6.09	0.005478
9	HSPB1_HUMAN	Heat shock protein β1	0.0285	0.0714	2.51	0.002229
10a	MLRM_HUMAN	Myosin regulatory light chain 2	0.8381	0.4336	−1.93	0.000007
10b	MLRN_HUMAN	Myosin regulatory light chain 2	0.6212	0.2070	−3.00	0.000001
11	ILK_HUMAN	Integrin-linked protein kinase	0.8299	0.4089	−2.03	0.000340
12	FIBA_HUMAN	Fibrinogen α chain precursor	0.1414	0.0549	−2.58	0.005281
13	AMPM1_HUMAN	Methionine aminopeptidase 1	0.2179	0.0866	−2.52	0.007359
14a	PLEK_HUMAN	Pleckstrin	0.6820	0.2551	−2.67	0.003865
14b	PLEK_HUMAN	Pleckstrin	0.6958	0.2313	−3.01	0.001464
15	CSRP1_HUMAN	Cysteine and glycine-rich protein 1	0.9050	0.4449	−2.03	0.000235
16	HBB_HUMAN	Hemoglobin subunit β	0.8877	2.3011	2.59	0.011719

The serial number listed here is identical to the respective number in Fig. 1, showing the position of the identified proteins. FC indicates the fold change between the mean spot intensities of MDS and healthy platelet samples.

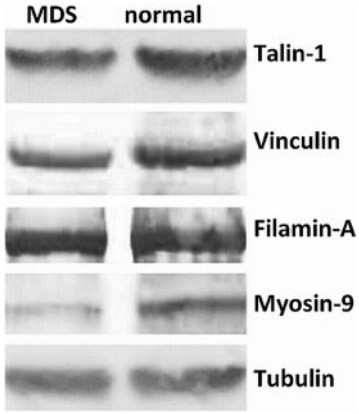

FIG. 2. **Western blot of platelet lysates from MDS patients and healthy donors.** The pooled platelet lysates from seven MDS patients and seven healthy donors show the decreased levels of Talin-1, Vinculin, Filamin-A, and Myosin-9 in MDS platelets.

Normal Surface Receptor Expression and Primary Activation in MDS Platelets—The aberrant platelet protein profile in MDS indicated an abnormal integrin signaling as a potential cause of defective platelet function in MDS. We therefore investigated the expression profiles of several integrins and other platelet surface receptors (GPIIIa, GPIIb, GPIb, GPVI, VLA-α_2, $P2Y_1$, and $P2Y_{12}$) and found no differences in the MFI of MDS and normal platelets ($n = 10$, Fig. 4*A*). Furthermore, we examined the very first step in platelet activation following agonist stimulation as we looked at the transient rise in $[Ca^{2+}]_i$ due to discharge from internal stores and found no differences between MDS and healthy donors ($n = 10$, Fig. 4*B*). As the calcium mobilization is critical for granule movement and secretion, we further analyzed granule release upon platelet activation using P-selectin. Our flow cytometric analysis also revealed no difference in the activation-dependent transport of P-selectin to the platelet

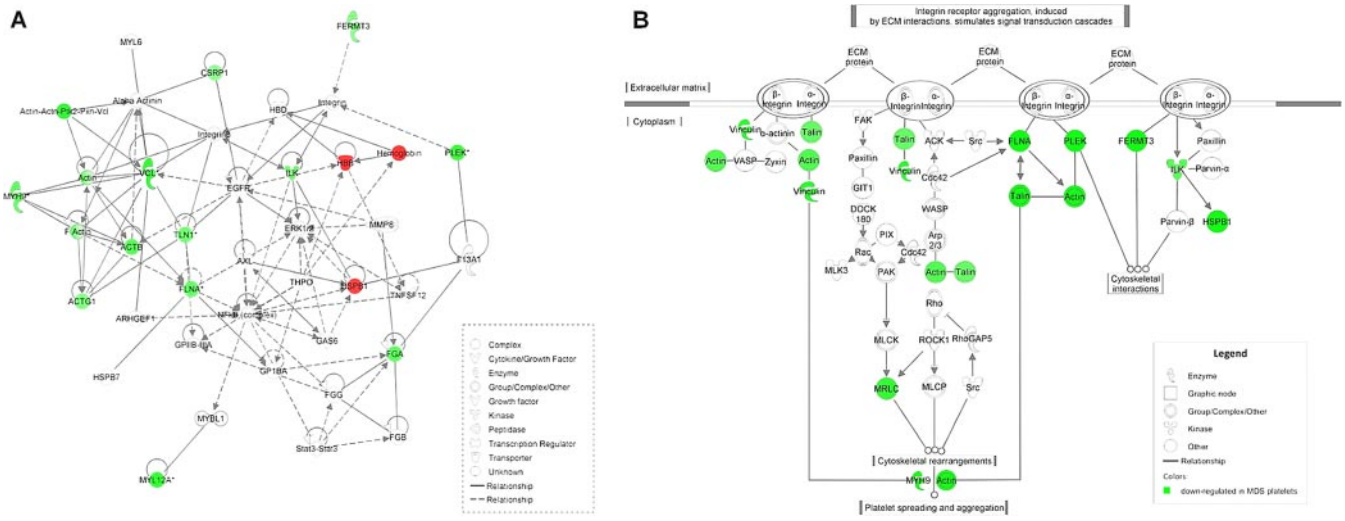

FIG. 3. **Ingenuity network and pathway analysis.** *A,* ingenuity network analysis using all identified proteins from our two-dimensional difference gel electrophoresis analysis. *B,* ingenuity pathway analysis of integrin signaling. Both show the up-regulated proteins in the MDS platelet in *red* and the down-regulated in *green*.

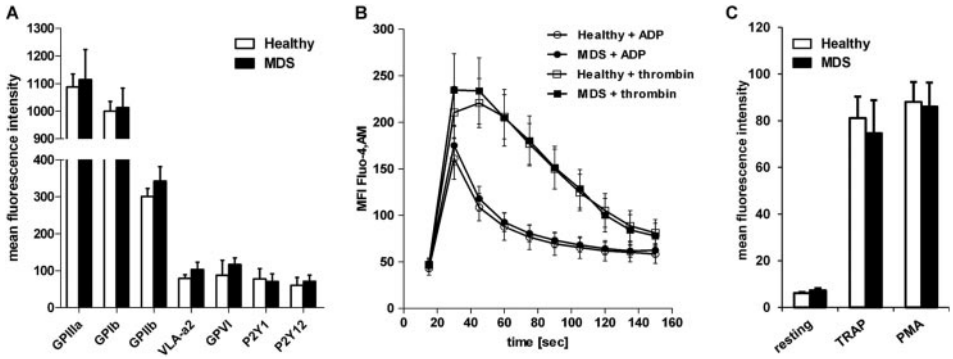

FIG. 4. **MDS platelet surface receptor characterization and primary activation.** *A,* flow cytometry analysis of platelets from MDS patients and normal donors shows no difference in surface levels of integrin $\alpha_{IIb}\beta_3$ (GPIIb/IIIa), ADP receptors $P2Y_1$ and $P2Y_{12}$, as well as collagen receptors GPVI and $\alpha_2\beta_1$ (*VLA-α2*) and von Willebrand factor receptor GPIb ($n = 10$). *B,* calcium mobilization from internal stores over time upon platelet activation with different agonists shows no difference between MDS and healthy donor platelets ($n = 10$). *C,* granule release upon platelet activation shows no difference between MDS and normal platelets ($n = 11$).

membrane in MDS platelets compared with their healthy counterparts ($n = 11$, Fig. 4*C*) indicating a normal primary activation of the MDS platelets.

MDS Platelets Show Insufficient Integrin $\alpha_{IIb}\beta_3$ Activation (Inside-out Signaling)—In the subsequent activation process, intact bidirectional signaling of integrin $\alpha_{IIb}\beta_3$ was a prerequisite for platelet activation and aggregation. To properly activate this receptor, Talin-1 and Kindlin-3 have to relocate from the cytoplasm to the cell membrane and bind to distinct domains of the integrin β_3. By utilizing FRET, we found that the energy transfer between Talin-1 and integrin $\alpha_{IIb}\beta_3$ upon activation with thrombin was markedly reduced in MDS platelets compared with normal ones ($n = 5$, $p < 0.05$), which indicates insufficient activation capacities of integrin $\alpha_{IIb}\beta_3$ (Fig. 5). To analyze the capability of this receptor to shift from its inactive low affinity to an active high affinity conformation, we assessed PAC-1 binding to this receptor by flow cytometry. PAC-1 exclusively recognizes the fibrinogen-binding site of integrin $\alpha_{IIb}\beta_3$ that is only accessible in its activated high affinity state (20). Following stimulation with TRAP as well as with agonist receptor-independent phorbol 12-myristate 13-acetate, PAC-1 binding was significantly reduced in MDS platelets ($n = 8$, $p < 0.05$ and 0.01, Fig. 6), demonstrating that in MDS platelets a significantly lower percentage of integrin $\alpha_{IIb}\beta_3$ was able to shift from its inactive to its active state. To rule out nonspecific nonsignaling-related defects of integrin $\alpha_{IIb}\beta_3$, such as a structural defect at the fibrinogen-binding site itself, we examined its PAC-1 binding capability following activation through Mn^{2+}, which is independent from intracellular signaling events. Here, we detected no differences between MDS and normal platelets ($n = 3$, Fig. 6) demonstrating principal functionality of the receptor itself.

Impaired Integrin $\alpha_{IIb}\beta_3$ Activation Leads to Inadequate Platelet Spreading and Aggregation—To further address po-

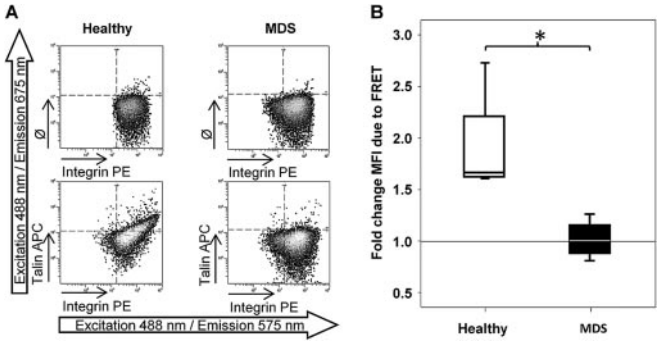

FIG. 5. **FRET analysis of talin-1 co-localization to the integrin β_3.** *A,* bi-parametric analysis of emissions at 575 nm (PE, *abscissa*) and 675 nm (APC, *ordinate*) after excitation at 488 nm of MDS and healthy platelets labeled with anti-integrin $\alpha_{IIb}\beta_3$ conjugated to PE (*upper panel*) and in combination with anti-talin-1 conjugated to APC (*lower panel*) showing the reduced emission at 675 nm in MDS. *B,* box plot showing the significantly reduced MFI at 675 nm after excitation with 488 nm in MDS platelets compared with normal donors ($n = 5$, $p < 0.05$).

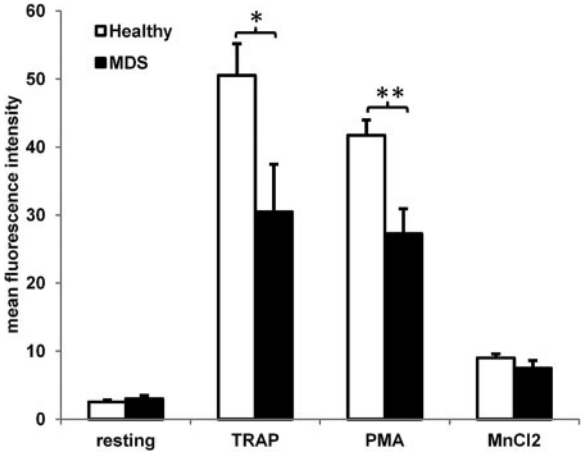

FIG. 6. **Flow cytometry analysis of MDS platelet activation.** MDS platelets show a significant decrease in their PAC-1 MFI following TRAP and phorbol 12-myristate 13-acetate stimulation resembling insufficient integrin $\alpha_{IIb}\beta_3$ activation ($n = 8$, $p < 0.05$ and 0.01). Mn^{2+}-stimulated platelets from MDS and normal donors show no differences with regard to PAC-1 binding ($n = 3$).

tential functional defects in MDS platelets, we analyzed outside-in signaling of the affected integrin $\alpha_{IIb}\beta_3$. Washed platelets of MDS patients and normal donors were exposed to immobilized fibrinogen. Following stimulation with thrombin, MDS platelets showed a spreading defect as they did mainly form filopodia but only few lamellipodia. Consequently, they failed to spread for up to 30 min, confirming the impaired outside-in signaling of integrin $\alpha_{IIb}\beta_3$ (Fig. 7*A*), which is in line with the reduced concentrations of Talin-1, Kindlin-3, Vinculin, Filamin-A, Actin, Myosin-9, and Myosin regulatory light chain 2 (MRLC2). Although MDS and normal platelets adhered similarly to the immobilized fibrinogen (integrin $\alpha_{IIb}\beta_3$-activation-independent), only 21% of the MDS platelets were fully spread after 30 min compared with 95% of healthy platelets ($n = 4$, $p < 0.001$, Fig. 7*B*). The impaired bidirectional signaling of integrin $\alpha_{IIb}\beta_3$ suggested a general defect in integrin-dependent platelet aggregation in MDS. However, shape change is not an essential prerequisite for aggregation, because adrenaline causes aggregation without shape change, and cytochalasin B inhibits shape change but not aggregation (21, 22). Therefore, we tested the ability of 58 MDS patients' platelets to aggregate in response to different agonists (Fig. 8*A*). In accordance with the observed defective integrin $\alpha_{IIb}\beta_3$ receptor activation in MDS, we found an insufficient aggregation in response to all four agonists (collagen $p < 0.001$, arachidonic acid $p < 0.01$, ADP $p < 0.01$, and ristocetin $p < 0.05$). Statistical χ^2 automatic interaction detection modeling of the dependence of the aggregation defect on multiple clinical parameters revealed that platelet count had the highest influence with 77% of the patients with platelets below 157,000/μl showing an aggregation defect compared with 21% of patients with higher platelet counts ($p < 0.001$, Fig. 8*B*). Other parameters that influenced aggregation capacity were the World Health Organization subtype and International Prognostic Scoring System (IPSS). Whereas patients with del(5q) showed a lower incidence of the aggregation defect compared with the other subtypes (22% *versus* 61%; $p < 0.05$), patients with chronic myelomonocytic leukemia (CMML) had a higher incidence (78% *versus* 51%, $p < 0.05$). Increasing IPSS correlated with increased aggregation defects ($p < 0.05$), with all high risk patients having the defect.

DISCUSSION

Platelet count-independent hemorrhages are a significant clinical problem in patients with MDS (3, 4). The presence of a functional platelet defect may aggravate bleeding complications in patients with low platelet counts and in general increase the complication rate during invasive procedures in MDS patients. So far, it has not been elucidated if abnormal hemostasis in MDS is systematic and if it follows a common platelet-intrinsic pathology.

Once platelets have been shed from megakaryocytes, they already contain most of the proteins required for their function. Therefore, quantitative platelet proteome analysis is an ideal tool to uncover platelet-intrinsic defects that may contribute to functional platelet defects. Our analysis of the MDS and healthy platelet proteomes revealed that the majority of proteins with different concentrations showed lower levels in MDS. This suggested that functional platelet defects in MDS may result from inadequate levels of proteins critical for platelet function. This hypothesis was further supported by our pathway/network analysis that showed that the majority of these lower concentrated proteins are essential for integrin signaling. Proper function of integrin $\alpha_{IIb}\beta_3$ is critical for platelet aggregation and hemostasis (13, 23). Among the proteins with lower levels in MDS were TAlin-1 and Kindlin-3, both binding to the β_3-subunit of integrin $\alpha_{IIb}\beta_3$, which is referred to as the common final step necessary for integrin activation

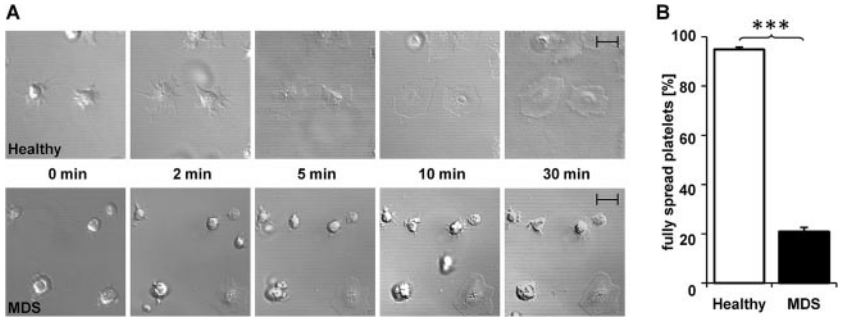

FIG. 7. **Defective spreading capacity of MDS platelets.** *A,* differential interference contrast microscopy images of one representative experiment out of four showing that thrombin-stimulated MDS platelets fail to completely spread over a continuous time period of 30 min forming only occasional filopodia/lamellipodia. Images were taken using a Zeiss LSM 510 META microscope in combination with a Plan-Neofluar 40×/1.3 oil differential interference contrast objective and processed by Zeiss LSM Image Browser Software Version 4.2.0.121. *Scale bar,* 5 μm. *B,* quantification of spread platelets in normal donors and MDS patients ($n = 4$). For each patient and normal donor, 100 platelets were counted after 30 min, and the *bar charts* represent the proportion of fully spread platelets showing a significantly lower proportion in MDS ($p < 0.001$).

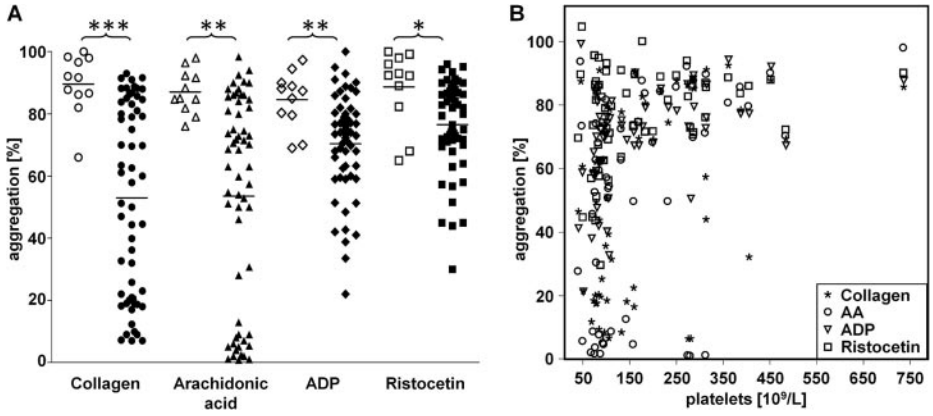

FIG. 8. **Integrin-dependent platelet aggregation defect in MDS.** *A,* compared with normal donor platelets, MDS platelets ($n = 58$) showed a significantly reduced aggregation in response to collagen and arachidonic acid ($p < 0.001$ and 0.01). Aggregation following ristocetin and ADP stimulation was also reduced ($p < 0.01$ and 0.05). *B,* scatter plot of platelet count *versus* aggregation capacity of 58 MDS patients showing that in patients with lower platelet counts (<157,000/μl) defective aggregation in response to collagen and arachidonic acid is more common ($p < 0.001$).

(14–16, 24–31). The proteins of the kindlin family and Talin-1 also establish major links between the β_3-subunit and the actin filaments of the cytoskeleton, which is necessary for initiation of subsequent platelet spreading (26, 27). Both of these signaling pathways are absolutely required for platelet function, and consistently, lack of Talin-1 or Kindlin-3 in platelets has been shown to abrogate integrin $\alpha_{IIb}\beta_3$ activation with loss of platelet spreading and aggregation *in vivo* (12, 13, 24). The reduced expression of these two proteins and their central role in integrin activation pointed toward abnormal integrin $\alpha_{IIb}\beta_3$ function in MDS. While surface receptor expression and early activation (calcium flux and granule release) did not differ between MDS and normal platelets, the integrin inside-out signaling upon activation was markedly reduced in MDS. Consequently, platelet spreading on immobilized fibrinogen was almost abolished in patients with MDS. Besides activation of integrin $\alpha_{IIb}\beta_3$, the ability to spread on immobilized fibrinogen requires the presence of Vinculin and cytoskeletal proteins such as Filamin-A, Actin, and Myosin-9, which were also expressed lower in MDS platelets. It has been shown that loss of Vinculin decreases cytoskeletal mechanics and spreading capacities (31, 32), and Filamin-A is responsible for the organization of F-actin into bundles and networks and the linkage of transmembrane receptors to the cytoskeleton (33, 34). The reduced expression of the major cytoskeletal proteins Actin and Myosin-9 also aggravates the poor spreading performance (35). This may explain why the spreading defect observed in MDS platelets was more severe than suggested solely by the incomplete integrin $\alpha_{IIb}\beta_3$ activation. Inside-out and thus Talin-1- or Kindlin-3-independent integrin $\alpha_{IIb}\beta_3$ functions such as adhesion to fibrinogen (36) or receptor activation following Mn^{2+} stimulation (37) remain intact in MDS platelets, pointing toward a specific integrin $\alpha_{IIb}\beta_3$ activation deficit in MDS originating from the reduced expression of essential signaling proteins such as Talin-1, Kindlin-3, Vinculin, Filamin-A, and Actin. With respect to their functional phenotype, MDS platelets mimic the platelet phenotype of conditional Talin-1 or Kindlin-3 knockout mice (12, 13, 24).

From a functional perspective, the impaired bidirectional integrin $\alpha_{IIb}\beta_3$ signaling in MDS suggests a general defect in integrin-dependent platelet aggregation. In line with this assumption, we found considerably decreased aggregation in response to the integrin-dependent agonists arachidonic acid and collagen when compared with normal donor platelets. We also found a diminished aggregation in response to ADP, although not as severe as against the other two. This could be

due to ADP's two P2Y receptors, of which only one is dependent on Chloride intracellular channel protein 1 (Clic1) that we found 3-fold down-regulated in MDS platelets. The absence of Clic1 was recently found to induce a lower ADP-stimulated platelet aggregation in mice that is dependent on the $P2Y_{12}$ but not the $P2Y_1$ receptor (38). We also detected a reduced response to ristocetin, which is independent of integrin $\alpha_{IIb}\beta_3$ function as it initiates platelet agglutination rather than aggregation (39). The reduced response to ristocetin observed in MDS patients might be explained by the lower levels of the cytoskeletal protein Myosin-9 as patients with inherited disorders involving the corresponding *MYH9* gene locus also present with a similarly reduced platelet aggregation capacity in response to ristocetin (40), as well as giant platelets (18, 41). The Myosin-9 deficiency in MDS platelets may have conceivably contributed to the increased mean platelet volume (>11 fl), a common phenomenon in MDS referred to as "giant" or "balloon-like" platelets (17), observed in the majority of MDS patients examined here. We observed the described effects consistently in patients with platelet counts ranging between 19,000 and 734,000/μl, whereas the aggregation defect positively correlated with platelet count, World Health Organization subtype, IPSS, and signs of bleeding. Although in our statistical analysis a lower platelet count (<157,000/μl) had the highest influence on the aggregation capacity, the average platelet count (89,000/μl) did not suggest aggregation defects in these patients thus indicating the existence of a functional defect.

Acknowledgments—We thank Waltraud Passlack and Annemarie Koch for excellent technical assistance.

* This work was supported by grants from Leukämie Lymphom Liga e.V. Düsseldorf and the Forschungskommission of the Heinrich-Heine-University, Düsseldorf, Germany.

S This article contains supplemental material.

‡ To whom correspondence should be addressed: Dept. of Hematology, Oncology, and Clinical Immunology, Heinrich-Heine-University Düsseldorf, Moorenstr. 5, 40225 Düsseldorf, Germany. Tel.: 49-211-8119606; Fax: 49-211-8104296; E-mail: julia.froebel@med.uni-duesseldorf.de.

REFERENCES

1. Germing, U., Strupp, C., Kündgen, A., Bowen, D., Aul, C., Haas, R., and Gattermann, N. (2004) No increase in age-specific incidence of myelodysplastic syndromes. *Haematologica* **89,** 905–910
2. van Lom, K., Houtsmuller, A. B., van Putten, W. L., Slater, R. M., and Löwenberg, B. (1999) Cytogenetic clonality analysis of megakaryocytes in myelodysplastic syndrome by dual-color fluorescence *in situ* hybridization and confocal laser scanning microscopy. *Genes Chromosomes Cancer* **25,** 332–338
3. Kantarjian, H., Giles, F., List, A., Lyons, R., Sekeres, M. A., Pierce, S., Deuson, R., and Leveque, J. (2007) The incidence and impact of thrombocytopenia in myelodysplastic syndromes. *Cancer* **109,** 1705–1714
4. Neukirchen, J., Blum, S., Kuendgen, A., Strupp, C., Aivado, M., Haas, R., Aul, C., Gattermann, N., and Germing, U. (2009) Platelet counts and haemorrhagic diathesis in patients with myelodysplastic syndromes. *Eur. J. Haematol.* **83,** 477–482
5. Pamphilon, D. H., Aparicio, S. R., Roberts, B. E., Menys, V. C., Tate, G., and Davies, J. A. (1984) The myelodysplastic syndromes-a study of haemostatic function and platelet ultrastructure. *Scand. J. Haematol.* **33,** 486–491
6. Mittelman, M., and Zeidman, A. (2000) Platelet function in the myelodysplastic syndromes. *Int. J. Hematol.* **71,** 95–98
7. Zeidman, A., Sokolover, N., Fradin, Z., Cohen, A., Redlich, O., and Mittelman, M. (2004) Platelet function and its clinical significance in the myelodysplastic syndromes. *Hematol. J.* **5,** 234–238
8. Girtovitis, F. I., Ntaios, G., Papadopoulos, A., Ioannidis, G., and Makris, P. E. (2007) Defective platelet aggregation in myelodysplastic syndromes. *Acta Haematol.* **118,** 117–122
9. Jennings, L. K. (2009) Role of platelets in atherothrombosis. *Am. J. Cardiol.* **103,** 4A–10A
10. Li, Z., Delaney, M. K., O'Brien, K. A., and Du, X. (2010) Signaling during platelet adhesion and activation. *Arterioscler. Thromb. Vasc. Biol.* **30,** 2341–2349
11. Knezevic, I., Leisner, T. M., and Lam, S. C. (1996) Direct binding of the platelet integrin αIIbβ3 (GPIIb-IIIa) to talin. Evidence that interaction is mediated through the cytoplasmic domains of both αIIb and β3. *J. Biol. Chem.* **271,** 16416–16421
12. Nieswandt, B., Moser, M., Pleines, I., Varga-Szabo, D., Monkley, S., Critchley, D., and Fässler, R. (2007) Loss of talin1 in platelets abrogates integrin activation, platelet aggregation, and thrombus formation *in vitro* and *in vivo*. *J. Exp. Med.* **204,** 3113–3118
13. Petrich, B. G., Marchese, P., Ruggeri, Z. M., Spiess, S., Weichert, R. A., Ye, F., Tiedt, R., Skoda, R. C., Monkley, S. J., Critchley, D. R., and Ginsberg, M. H. (2007) Talin is required for integrin-mediated platelet function in hemostasis and thrombosis. *J. Exp. Med.* **204,** 3103–3111
14. Vinogradova, O., Velyvis, A., Velyviene, A., Hu, B., Haas, T., Plow, E., and Qin, J. (2002) A structural mechanism of integrin α(IIb)β(3) "inside-out" activation as regulated by its cytoplasmic face. *Cell* **110,** 587–597
15. Ye, F., Hu, G., Taylor, D., Ratnikov, B., Bobkov, A. A., McLean, M. A., Sligar, S. G., Taylor, K. A., and Ginsberg, M. H. (2010) Recreation of the terminal events in physiological integrin activation. *J. Cell Biol.* **188,** 157–173
16. Petrich, B. G., Fogelstrand, P., Partridge, A. W., Yousefi, N., Ablooglu, A. J., Shattil, S. J., and Ginsberg, M. H. (2007) The antithrombotic potential of selective blockade of talin-dependent integrin αIIbβ3 (platelet GPIIb-IIIa) activation. *J. Clin. Invest.* **117,** 2250–2259
17. Widell, S., and Hast, R. (1987) Balloon-like platelets in myelodysplastic syndromes-a feature of dysmegakaryopoiesis? *Leuk. Res.* **11,** 747–752
18. Seri, M., Cusano, R., Gangarossa, S., Caridi, G., Bordo, D., Lo Nigro, C., Ghiggeri, G. M., Ravazzolo, R., Savino, M., Del Vecchio, M., d'Apolito, M., Iolascon, A., Zelante, L. L., Savoia, A., Balduini, C. L., Noris, P., Magrini, U., Belletti, S., Heath, K. E., Babcock, M., Glucksman, M. J., Aliprandis, E., Bizzaro, N., Desnick, R. J., and Martignetti, J. A. (2000) Mutations in MYH9 result in the May-Hegglin anomaly, and Fechtner and Sebastian syndromes. The May-Hegglin/Fechtner Syndrome Consortium. *Nat. Genet.* **26,** 103–105
19. Lehr, S., Kotzka, J., Avci, H., Knebel, B., Muller, S., Hanisch, F. G., Jacob, S., Haak, C., Susanto, F., and Muller-Wieland, D. (2005) Effect of sterol regulatory element binding protein-1a on the mitochondrial protein pattern in human liver cells detected by 2D-DIGE. *Biochemistry* **44,** 5117–5128
20. O'Toole, T. E., Mandelman, D., Forsyth, J., Shattil, S. J., Plow, E. F., and Ginsberg, M. H. (1991) Modulation of the affinity of integrin αIIbβ3 (GPIIb-IIIa) by the cytoplasmic domain of αIIb. *Science* **254,** 845–847
21. White J. G. (1971) Platelet Microtubules and Microfilaments: Effects of Cytochalasin B on Structure and Function. *Caen J. Platelet Aggregation,* 15–52
22. Mustard, J. F., and Packham, M. A. (1970) Factors influencing platelet function: adhesion, release, and aggregation. *Pharmacol. Rev.* **22,** 97–187
23. Peerschke, E. I., Zucker, M. B., Grant, R. A., Egan, J. J., and Johnson, M. M. (1980) Correlation between fibrinogen binding to human platelets and platelet aggregability. *Blood* **55,** 841–847
24. Moser, M., Nieswandt, B., Ussar, S., Pozgajova, M., and Fässler, R. (2008) Kindlin-3 is essential for integrin activation and platelet aggregation. *Nat. Med.* **14,** 325–330
25. Patil, S., Jedsadayanmata, A., Wencel-Drake, J. D., Wang, W., Knezevic, I., and Lam, S. C. (1999) Identification of a talin-binding site in the integrin β_3 subunit distinct from the NPLY regulatory motif of post-ligand binding functions. The talin N-terminal head domain interacts with the membrane-proximal region of the β_3 cytoplasmic tail. *J. Biol. Chem.* **274,**

28575–28583
26. Tadokoro, S., Shattil, S. J., Eto, K., Tai, V., Liddington, R. C., de Pereda, J. M., Ginsberg, M. H., and Calderwood, D. A. (2003) Talin binding to integrin β tails: a final common step in integrin activation. *Science* **302,** 103–106
27. Larjava, H., Plow, E. F., and Wu, C. (2008) Kindlins: essential regulators of integrin signalling and cell-matrix adhesion. *EMBO Rep.* **9,** 1203–1208
28. Ussar, S., Wang, H. V., Linder, S., Fässler, R., and Moser, M. (2006) The Kindlins: subcellular localization and expression during murine development. *Exp. Cell Res.* **312,** 3142–3151
29. Ziegler, W. H., Gingras, A. R., Critchley, D. R., and Emsley, J. (2008) Integrin connections to the cytoskeleton through talin and vinculin. *Biochem. Soc. Trans.* **36,** 235–239
30. Feng, S., Reséndiz, J. C., Lu, X., and Kroll, M. H. (2003) Filamin A binding to the cytoplasmic tail of glycoprotein Ibα regulates von Willebrand factor-induced platelet activation. *Blood* **102,** 2122–2129
31. Rodríguez Fernández, J. L., Geiger, B., Salomon, D., and Ben-Ze'ev, A. (1993) Suppression of vinculin expression by antisense transfection confers changes in cell morphology, motility, and anchorage-dependent growth of 3T3 cells. *J. Cell Biol.* **122,** 1285–1294
32. Goldmann, W. H., Schindl, M., Cardozo, T. J., and Ezzell, R. M. (1995) Motility of vinculin-deficient F9 embryonic carcinoma cells analyzed by video, laser confocal, and reflection interference contrast microscopy. *Exp. Cell Res.* **221,** 311–319
33. Robertson, S. P. (2005) Filamin A: phenotypic diversity. *Curr. Opin. Genet. Dev.* **15,** 301–307
34. van der Flier, A., and Sonnenberg, A. (2001) Structural and functional aspects of filamins. *Biochim. Biophys. Acta.* **1538,** 99–117
35. Léon, C., Eckly, A., Hechler, B., Aleil, B., Freund, M., Ravanat, C., Jourdain, M., Nonne, C., Weber, J., Tiedt, R., Gratacap, M. P., Severin, S., Cazenave, J. P., Lanza, F., Skoda, R., and Gachet, C. (2007) Megakaryocyte-restricted MYH9 inactivation dramatically affects hemostasis while preserving platelet aggregation and secretion. *Blood* **110,** 3183–3191
36. Savage, B., Shattil, S. J., and Ruggeri, Z. M. (1992) Modulation of platelet function through adhesion receptors. A dual role for glycoprotein IIb-IIIa (integrin αIIbβ3) mediated by fibrinogen and glycoprotein Ib-von Willebrand factor. *J. Biol. Chem.* **267,** 11300–11306
37. Mould, A. P., Askari, J. A., Barton, S., Kline, A. D., McEwan, P. A., Craig, S. E., and Humphries, M. J. (2002) Integrin activation involves a conformational change in the α1 helix of the β subunit A-domain. *J. Biol. Chem.* **277,** 19800–19805
38. Qiu, M. R., Jiang, L., Matthaei, K. I., Schoenwaelder, S. M., Kuffner, T., Mangin, P., Joseph, J. E., Low, J., Connor, D., Valenzuela, S. M., Curmi, P. M., Brown, L. J., Mahaut-Smith, M., Jackson, S. P., and Breit, S. N. (2010) Generation and characterization of mice with null mutation of the chloride intracellular channel 1 gene. *Genesis* **48,** 127–136
39. Burgess-Wilson, M. E., Cockbill, S. R., Johnston, G. I., and Heptinstall, S. (1987) Platelet aggregation in whole blood from patients with Glanzmann's thrombasthenia. *Blood* **69,** 38–42
40. Redman, R., Shunkwiler, S. M., Harris, N. S., Kedar, A., and Clapp, W. L. (2008) Sebastian syndrome with abnormal platelet response to ristocetin. *Lab. Hematol.* **14,** 19–23
41. Eckly, A., Strassel, C., Freund, M., Cazenave, J. P., Lanza, F., Gachet, C., and Léon, C. (2009) Abnormal megakaryocyte morphology and proplatelet formation in mice with megakaryocyte-restricted MYH9 inactivation. *Blood* **113,** 3182–3189